

1 Search for dark matter with liquid argon

C. AMSLER, V. BOCCONE, H. CABRERA¹, S. HORIKAWA, C. REGENFUS, J. ROCHET, and M. THOMANN²

In collaboration with:

CIEMAT, ETHZ, Soltan Institute (Warsaw), Universities of Granada and Sheffield

(ArDM Collaboration)

We are building a one ton liquid argon time projection chamber to detect recoil nuclei from the scattering of Weak Interacting Massive Particles. WIMPs (in particular the lightest supersymmetric particle, the neutralino), are among the favorite candidates for the missing non-baryonic matter in the universe. Details on the experiment can be found in our previous annual reports.

In 2007 the Zurich group concluded its laboratory development program for the light readout system and the ArDM collaboration started to assemble the full-scale one ton apparatus. A sketch of the detector is shown in Fig. 1.1. The working principle is as follows: in

liquid argon a WIMP collision leading to 30 keV nuclear recoils produces about 400 VUV (128 nm) photons, together with a few free electrons. The latter are drifted in a strong vertical electric field and are detected in the gas phase by a large electron multiplier above the surface of the liquid, while the VUV scintillation light is shifted into blue light by a wavelength shifter (WLS) and detected by cryogenic photomultipliers at the bottom of the vessel.

From extensive tests performed by our group we concluded that the highest light collection efficiency would be achieved with WLSs made of a $254\ \mu$ thick Teflon fabric (Tetratex) coated with $\approx 1\ \text{mg}/\text{cm}^2$ tetraphenyl butadiene (TPB) (1) (see below). We constructed a large evaporation chamber capable of coating a 1.4 m long and 0.3 m wide sheet of Tetratex. Twelve sheets were coated to cover the cylindrical side walls inside the electric field shapers (Fig. 1.2). The light detection system consists of fourteen 8" hemispherical PMTs in a staggered arrangement at the bottom of the vessel (Fig. 1.3). We have investigated PMTs for their functionality and quantum efficiency at low temperature. The best result was obtained with Hamamatsu PMTs (R5912-MOD) manufactured with Pt-underlay. A light but sufficiently strong mechanical support was constructed to withstand the buoyant force ($\approx 1\ \text{kN}$) acting on the PMTs in liquid argon. Eight PMTs were installed for readout tests. The PMT glass was coated with a thin wavelength shifting layer of a transparent TPB-paraloid compound to increase the VUV light

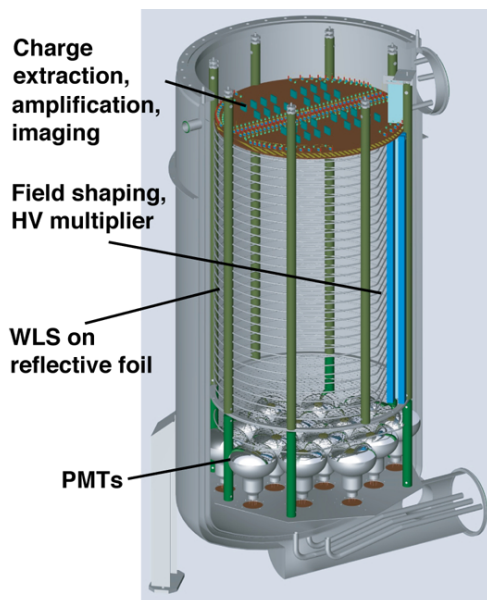


Figure 1.1: Sketch of the ArDM detector.

¹Master student

²Bachelor student

yield. Vacuum feedthroughs, cables for the high voltage and signal lines were installed, as well as parts of the data acquisition system.

The ratio of primary scintillation light to ionization charge collected after a given drifttime in an external electric field is different for nuclear recoils and minimum ionizing particles, being very high for the former, due to quenching. This provides the main discrimination between WIMPs and background. In liquid, on the other hand, the VUV photons are produced by ionization from the spin singlet and triplet states of the excited dimer A_2^* which have different lifetimes ($\tau = 7$ ns, resp. 1.6 μ s in liquid). These states are populated differently according to the excitation process: for heavy ionization (such as nuclear recoils) the singlet dominates, while for minimum ionizing particles (such as electrons) the triplet dominates. Hence the discrimination of decay time allows a further separation between WIMP induced recoils and background from γ or electrons.

A considerable effort was devoted in 2007 to measure the mean decay lives of the fast (12 ns) and slow (3.2 μ s) components of argon luminescence in argon gas at NTP (which are different from liquid) and to determine the population ratio between the slow and fast components. We used a ^{210}Pb -source emitting 5.3 MeV α -particles and 1.2 MeV electrons. This work initiated in ref. (2) is the subject of a recent publication (3). Figure 1.4 shows for instance that the mean life of the slow component strongly depends on argon purity.

We have also determined that the fast decaying component in gaseous argon at NTP stems from UV-light from the so-called (4) third continuum above 160 nm, while the slow component is due to 128 nm photons from the second continuum. This appears to be in contrast to liquid in which both components are due to 128 nm VUV-photons. The measurement was performed by inserting a thin quartz plate in

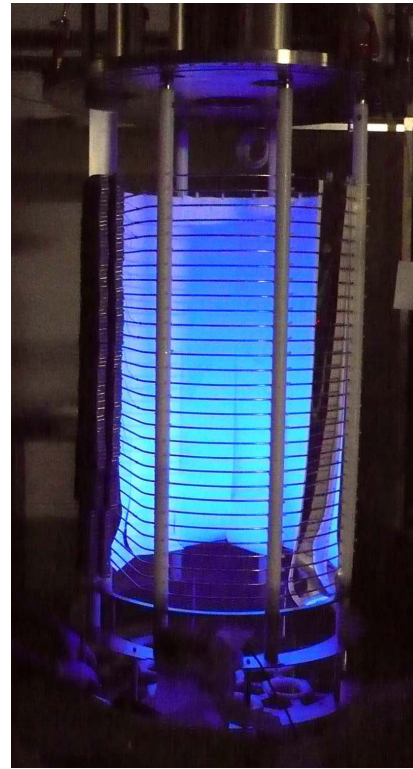


Figure 1.2: HV divider, WLS foils and photomultipliers under UV illumination.



Figure 1.3: PMT support structure built by our group with three of the fourteen 8" (Hamamatsu R5912-MOD) PMTs.

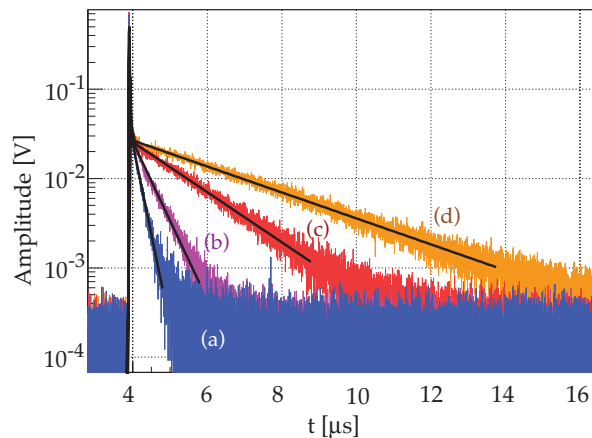


Figure 1.4: Time distribution from an α -source in gaseous argon as a function of contaminating residual air pressure for 10^{-2} (a), 10^{-3} (b), 2.3×10^{-4} (c) and 10^{-5} mbar (d) (from [3]).

front of the PMT photocathode to absorb radiation below 200 nm. Figure 1.5 shows that the fast component is not affected, while the slow component is absorbed (3).

Similar measurements were made in liquid argon (5). In liquid we noticed that the light yield was slowly decreasing with time after liquefaction. However, the decay time of the second component ($\tau = 1.6 \mu\text{s}$) was not affected. The origin of this effect is not understood yet, but could be interpreted either as due to the slow cooling of the dynodes (poor heat conductance of the PMT leads) or due to impurities which are absorbing the UV-light.

We also measured the light yield dependence on the WLS thickness of evaporated specular reflectors foils. The measurements were made with a small cell containing gaseous argon at atmospheric pressure. Two materials were selected, Tetratex and ESR-foils from 3M, and the optimum thickness of the TPB layer on the reflector was determined experimentally (1). The best conversion efficiency, uniformity and reproducibility were achieved by evaporating TPB on the reflector. Several disks of ESR foils (diameter 70 mm) were covered with TPB layers of different thick-

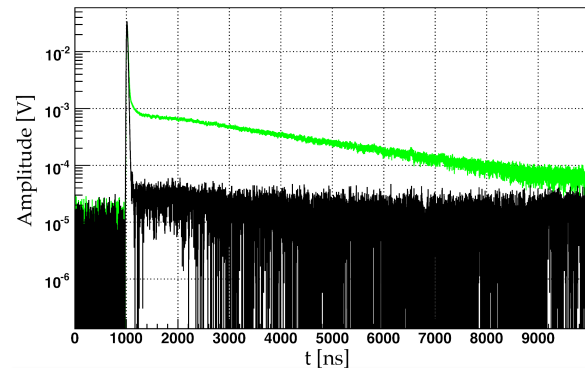


Figure 1.5: Time distribution without (green) and with (black) absorbing quartz plate.

nesses. The TPB thickness was determined by weighing the disks before and after evaporation. The increase in brightness with TPB thickness is apparent under UV illumination (300 nm) (Fig. 1.6). The response to 128 nm light was determined using scintillation light from gaseous argon and an α -source. The light yield of the slow component ($3.2 \mu\text{s}$ in gas) is shown in Fig. 1.7 as a function of thickness. The data are consistent with a saturat-

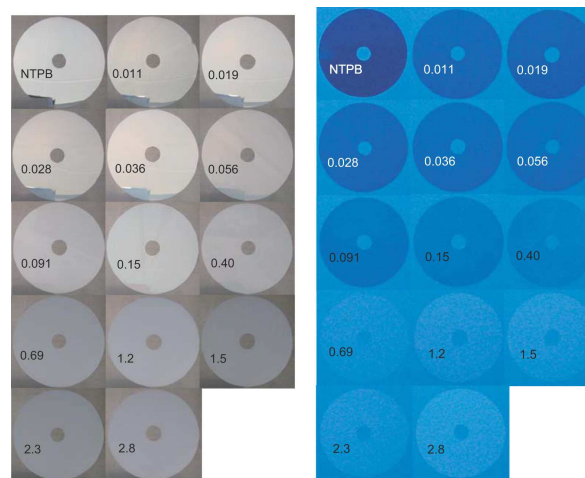


Figure 1.6: Disks of ESR-foils covered with TPB under ambient and UV light.

tion of VUV conversion efficiency above $1 \text{ mg} \cdot \text{cm}^{-2}$. Tetratex coated with $1 \text{ mg} \cdot \text{cm}^{-2}$ TPB was finally chosen for the one ton detector.

As mentioned above, impurities in argon strongly reduce the lifetime of the slow scintillation component. We have therefore built a liquid-argon purity monitor based on the measurement of the lifetime of the triplet excimer state. A small liquid argon cell containing a ^{210}Pb -source emitting both α and β is viewed by a photomultiplier with MgF_2 window and CsTe photocathode which is sensitive to $128 \text{ } \mu\text{m}$ VUV-photons (quantum efficiency $\sim 20\%$). Figure 1.8 shows the correlation between the fraction R of the fast ($< 50 \text{ ns}$) scintillation component and the total pulse height. The α -signal is clearly separated from the β -signal and noise. The decay time distribution is shown in Fig. 1.9 for α -particles. A simple exponential fit leads to a mean life of $\sim 470 \text{ ns}$ for the slow component (while $1.6 \text{ } \mu\text{s}$ is expected) and hence indicates a sizeable impurity contamination in the liquid.

The ArDM detector is being assembled at CERN for preliminary readout measurements. We envisage to first install the detector in one of the former LEP pits (OPAL area) for background studies, before moving to a deep underground site.

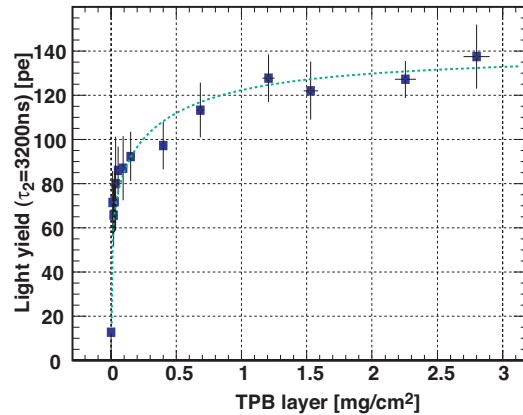


Figure 1.7: Number of photoelectrons (pe) as a function of WLS thickness.

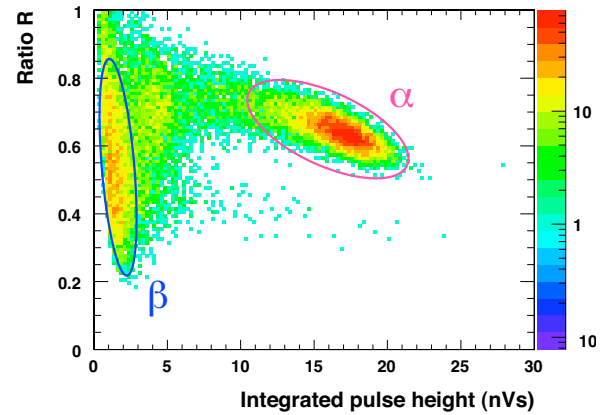


Figure 1.8: Ratio of the fast ($< 50 \text{ ns}$) signal to the total signal in liquid argon vs. total signal in the purity monitor.

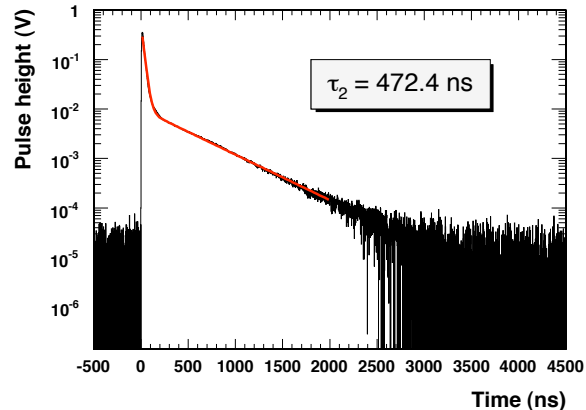


Figure 1.9: Decay time distribution for α -particles.

- [1] H. Cabrera, Master Thesis, Universität Zürich (2007).
- [2] A. Büchler, Bachelor Thesis, Universität Zürich (2006).
- [3] C. Amsler *et al.*, Journal of Instrumentation **3** (2008) P02001.
- [4] W. Krötz *et al.*, Phys. Rev. **A** **43** (1991) 6089.
- [5] M. Thomann, Bachelor Thesis, Universität Zürich (2008).